JMEPEG (2009) 18:433–437
DOI: 10.1007/s11665-008-9275-8

1059-9495/$19.00

# Investigation on Addition of Kaolinite on Sintering Behavior and Mechanical Properties of $B_4C$

*H.R. Baharvandi and A.M. Hadian*

*(Submitted November 10, 2007; in revised form May 28, 2008)*

**The objective of the present investigation was to study the effect of kaolinite addition on sintering behavior and mechanical properties of pressureless sintered $B_4C$ ceramic. Different amounts of kaolinite, mainly 5 to 30 wt.%, were added to the base material. The in situ reaction of kaolinite with $B_4C$ generates SiC and $Al_2O_3$, which aid the sintering process and permit pressureless sintering at temperatures between 2050 and 2150 °C. Addition of 30 wt.% kaolinite and sintering at 2150 °C resulted in improving the density of the samples to about 98.5% of the theoretical density. The composite samples exhibited very good mechanical properties (hardness, flexural strength, and fracture toughness). As wt.% Kaolinite increases, strength and toughness increase, and hardness first increases and then decreases.**

**Keywords** boron carbide, kaolinite, sintering

## 1. Introduction

Due to their outstanding properties such as high hardness, wear resistance, low specific weight, and resistance to chemical attacks, boron carbide ($B_4C$) ceramics are regarded as having great potential for applications in wear-resistant parts and for armor materials (Ref 1-21). However, the use of monolithic boron carbide is limited by its low strength, low toughness, poor sinterability and machinability. Since $B_4C$ is very difficult to densify to higher than 80% of the theoretical density (TD), a variety of Elements and compounds are added to $B_4C$ as sintering aids (Ref 1-14).

Nonoxide ceramics such as SiC (Ref 1-3), TiC (Ref 4), C (Ref 5-6), and $TiB_2$ (Ref 14-20) have also been found to be very effective as sintering aids for $B_4C$. Metallic sintering aids such as Al (Ref 7), Si (Ref 11), Ti (Ref 12), Mg, and Fe are frequently added to provide a medium for liquid-phase sintering. Metallic phases at the grain boundaries generally deteriorate the unique properties of hard ceramics. However, in these cases, either large amounts of second phase or very high sintering temperatures are required for full densification (Ref 1-3). It has been frequently observed that small amounts of oxides such as $Al_2O_3$ (Ref 18, 19), $TiO_2$ (Ref 17, 20), and $Cr_2O_3$ (Ref 21) are very effective in improving the sinterability of $B_4C$. Since these powders must be very fine and with high purity to improve sintering, they are generally very expensive.

In the present study, the effect of kaolinite addition on densification behavior of $B_4C$ has been investigated. The selection of this sintering aid was due to the fact that this is an abundant material, which converts to $Al_2O_3$ and SiC during the course of sintering.

Other properties, such as hardness and fracture toughness of $B_4C$, have been measured and correlated with the variations in density and composition of the sintered bodies.

**H.R. Baharvandi**, University of Malek Ashtar, Tehran, Iran; and **A.M. Hadian**, School of Metallurgy and Materials, Faculty of Engineering, University of Tehran, Tehran, Iran. Contact e-mail: Hrbahar@ut.ac.ir.

## 2. Experimental Procedure

The starting materials used in the present study consisted of high-purity $B_4C$ (B:C ratio of 3.8-3.9) and kaolinite powder ($Al_2Si_2O_5(OH)_4$) from green world company, China. The average particle size of $B_4C$ powder was measured using a laser particle size analyzer (CILAS 1064, France) and found to be about 1.33 μm. The specific surface area of this powder was measured to be 6.64 $m^2/g$ (using a BET instrument, model NOVA 1200). For removing water, kaolinite powder was preheated to 550 °C for 1 h. Different amounts of preheated kaolinite, mainly 5, 10, 15, 20, 25, and 30 wt.%, were added as the sintering aid. Mixed $B_4C$ and kaolinite powders were ball milled in isopropyl alcohol for 8 h using high purity $Al_2O_3$ balls. The mixture was then dried in a rotary vacuum evaporator and passed through a 60 mesh screen. The powder mixtures were cold pressed under 80 MPa pressure into samples having $3 \times 3 \times 60$ $mm^3$ volume. The green samples were then sintered at 2050 and 2150 °C using a microprocessor controlled graphite element vacuum furnace. After evacuation, the furnace was filled with Ar gas and heated up to the sintering temperature at a heating rate of 10 °C/min. After holding for 1 hr at the temperature, the furnace was shut down and allowed to cool to room temperature naturally.

For microstructural examination, dense sintered bodies were surface ground and polished with diamond paste down to 1 μm surface finish. The polished surfaces were then electrolytically etched in a 0.1 M KOH solution at a current density of 0.1 $A/cm^2$ for 10-20 s. Microstructures of the specimens were observed using scanning electron microscope (SEM, CAMSCAN MV2300) and the microstructural constituents identified by X-ray diffraction (XRD, PHILIPS PW 1830) method. The density was

**Table 1 Phase composition after sintering at 2050°C**

| | Wt.% of kaolinite | | |
|---|---|---|---|
| Phase | 10 | 20 | 30 |
| $Al_2O_3$ (wt.%) | 4.85 | 9.8 | 14.8 |
| SiC (wt.%) | 5.9 | 11.6 | 17.9 |

measured by Archimedes method (Ref 22). The Al and Si concentrations in the fired specimens and some green compacts were determined using wet chemistry and atomic adsorption spectroscopy methods. An approximate theoretical density was calculated for the various ternary compositions of $B_4C$-$Al_2O_3$-SiC system. This approximation was based on the measured Al and Si concentrations from which the volumetric percentage of phases was derived. Based on this method, the composition of sintered samples at 2050 °C for 1 h was determined (Table 1). The same method has already been used for the $B_4C$-$ZrO_2$ system (Ref 10).

The flexural strength was measured by four-point flexural test method using a universal testing machine with a crosshead speed of 0.5 mm/min. The inner and outer spans of the jig were 20 and 40 mm, respectively. Samples were cut to volume of $3 \times 4 \times 45$ mm$^3$ and ground with an 800 grit diamond grinding wheel. The tensile side of the specimens was polished with diamond paste down to 1 μm finish (Ref 23-25). To measure the hardness, a Vickers indentor was used with a load of 1.96 N. The fracture toughness of the specimens was determined by the indentation strength method (Ref 26, 27). Small surface cracks of controlled size and shape can be readily induced in most ceramics by sharp hardness indenters (Fig. 1).

After indenting, the center of a polished surface beam specimen at 98 N with a Vickers indentor for 15 s, the fracture strength was measured with the 4-point flexural configuration, based on (Eq 1) (Ref 24-26).

$$K_{IC} = \eta(E/H)^{n/4}(\sigma_f p^{1/3})^{3/4} \quad \text{(Eq 1)}$$

where $K_{IC}$, $\sigma_f$, $p$, $E$, and $H$ are fracture toughness, fracture strength, applied load, young module, and vickers hardness, respectively. The factor $\eta$ depends on the residual stress factor $\chi$ and it was determined empirically as $0.59 \pm 0.12$ by Chantikul et al. (Ref 26, 27).

## 3. Results and Discussion

Figure 2 shows XRD patterns of $B_4C$ with kaolinite before and after sintering at 2150 °C for 1 h. These results indicate that a reaction between $B_4C$ and kaolinite has occurred during sintering. Before sintering, there are only $B_4C$ and kaolinite peaks as shown in Fig. 2. After sintering, SiC and $Al_2O_3$ peaks were detected and the kaolinite peaks disappeared, indicating that there was a reaction between the $B_4C$ and kaolinite to produce these phases.

Figures 3 and 4 show SEM images indicating the influence of kaolinite on densification of boron carbide. The figures show that monolithic $B_4C$ sintered at 2050 (Fig. 3a) and 2150°C (Fig. 4a) is not fully densified. Addition of 30 wt.% kaolinite to the starting powder results in higher density.

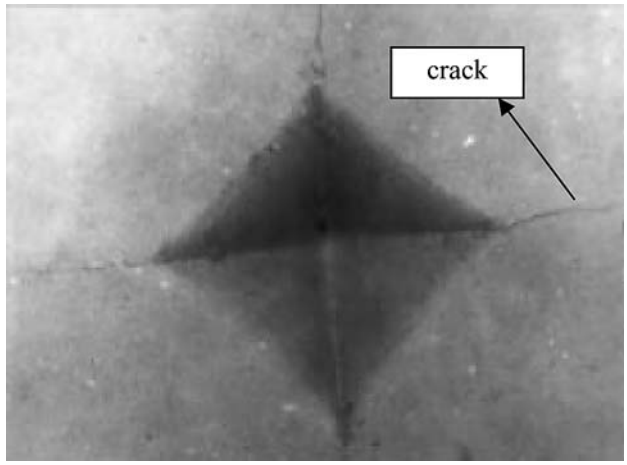


**Fig. 1** Small surface cracks induced in ceramic by sharp Vickers hardness (Ref 27)

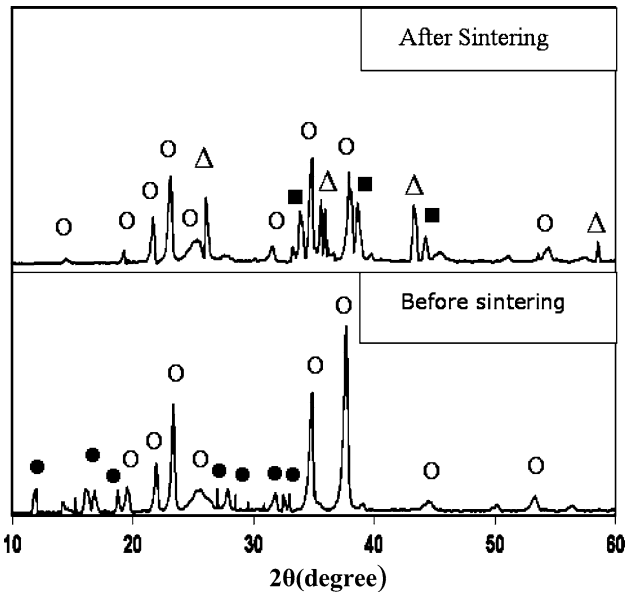


**Fig. 2** XRD patterns of $B_4C$ with 10 wt.% kaolinite before and after sintering at 2050 °C for 1 h ( ○ $B_4C$; • Kaolinite; ■ SiC; Δ $Al_2O_3$)

This is due to the fact that at sintering temperature, the $SiO_2$ content of kaolinite converts to SiC while $Al_2O_3$ remains at grain boundaries. Formation of these phases was detected by XRD analysis.

At about 1100 °C, kaolinite decomposes to mullite ($3Al_2O_3$,$2SiO_2$) and $SiO_2$, which turn into liquid at temperatures below 2000 °C. These liquid phases at sintering temperature react with $B_4C$ to form SiC and $Al_2O_3$. Therefore, transient liquid phase sintering occurs in this system, which allows for pressureless full density processing and property improvement. The effect of the presence of new phases on sintering behavior of $B_4C$ has been studied by a number of researchers (Ref 1, 12, 19). The primary effect is considerable increase in relative density (Fig. 3b and 4b), which is due to enhanced mass transport within these phases or reaction products at the grain boundaries. This improves such properties as hardness and fracture toughness (Ref 19).

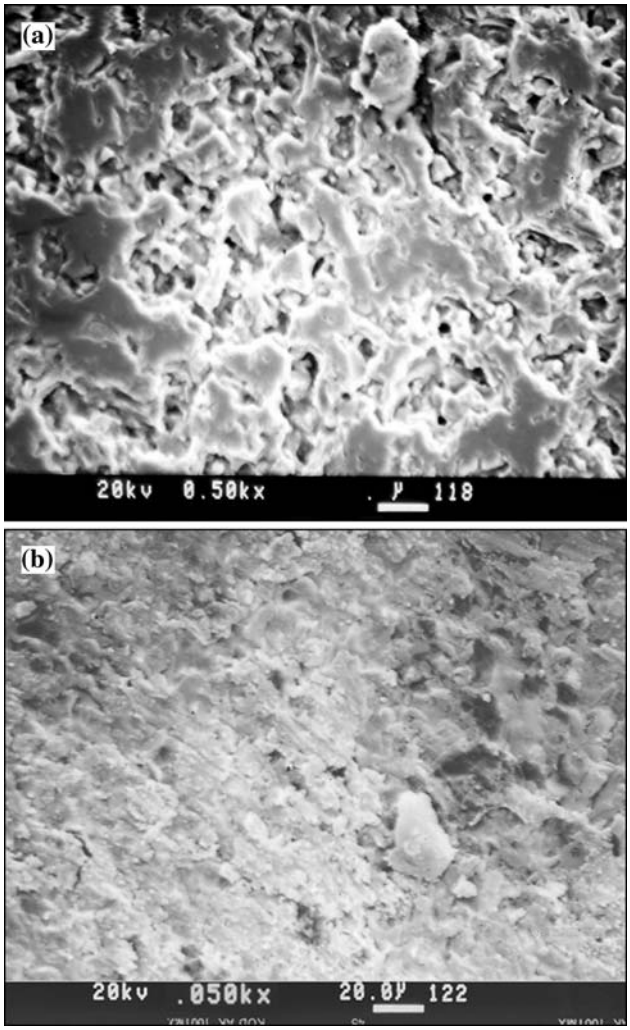


**Fig. 3** SEM micrographs of samples sintered at 2050 °C for 1 h (a) $B_4C$ (b) and $B_4C$-30 wt.% kaolinite

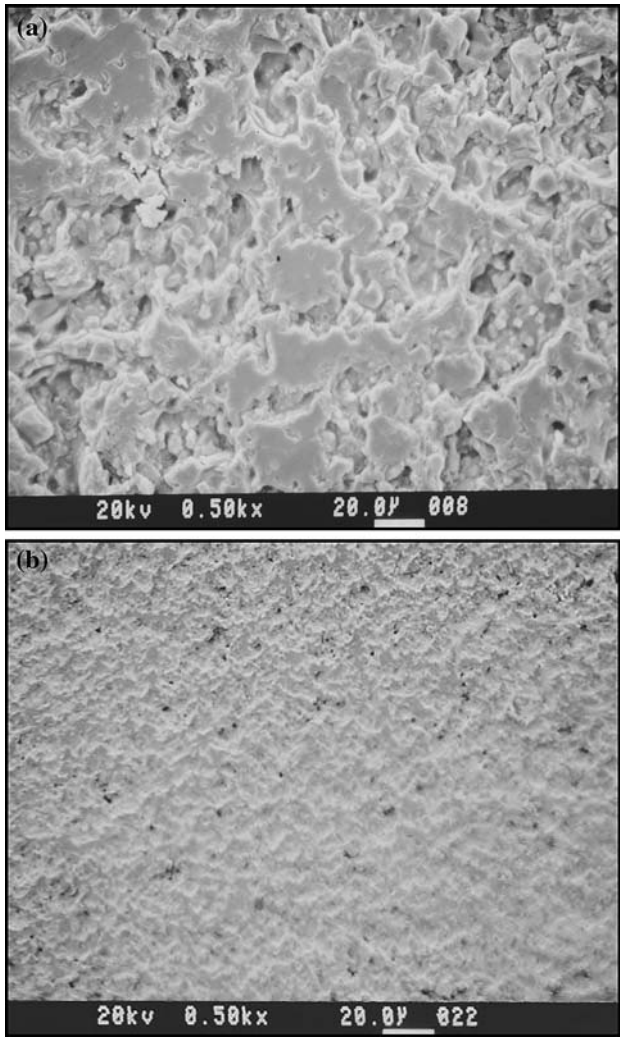


**Fig. 4** SEM micrographs of samples sintered at 2150 °C for 1 h (a) $B_4C$ (b) and $B_4C$-30 wt.% kaolinite

The effect of kaolinite addition on relative density of the samples sintered at 2050 and 2150 °C as a function of kaolinite percentage is shown in Fig. 5. As can be seen from the figure, the density increases with increasing kaolinite in the starting powder. The addition of 30 wt.% kaolinite has increased the relative density from 78 to 98.5% of TD. The increasing density will improve the mechanical properties as well. Figure 6 illustrates the variation of hardness as a function of the amount of kaolinite in the compositions. As can be seen, the highest hardness value obtained was about 31 GPa for the samples having 15% kaolinite in their compositions and sintered at 2150 °C. This value is very close to the hardness of fully densified pure $B_4C$ materials (31-35 GPa depending on sintering temperature and method).

The reduction of hardness in samples having more than 20 wt.% kaolinite is due to the presence of less hard phases such as $Al_2O_3$ and SiC as reaction products in the samples, compared to $B_4C$.

Therefore, the increase of kaolinite content will result in lowering the hardness. Moreover, it was found that the hardness of the samples sintered at 2150 °C is higher than that of the samples sintered at 2050 °C possibly due to greater densification.

Figure 7 illustrates the effect of kaolinite addition on flexural strength of the samples. From the figure, it is evident that by increasing the kaolinite up to 30 wt.%, flexural strength of the samples increases, which is possibly due to the higher density and the presence of higher compression stress on $B_4C$ grains. As can be seen, the flexural strength of the samples sintered at 2150 °C is higher than that of the samples sintered at 2050 °C. The same behavior has been seen for fracture toughness in Fig. 8.

The effect of density on improvement of mechanical properties is related to the amount of porosity and its role on such properties. Therefore, by decreasing the porosity, the mechanical properties, except hardness, will enhance. The hardness increases up to 20 wt.% kaolinite and then decreases up to 30 wt.% kaolinite. It is suggested that the lower hardness of the samples having higher amount of kaolinite is related to higher amount of $Al_2O_3$ and $MgB_2$ in such samples. The effect of density on improvement of mechanical properties has been reported by Kim for $B_4C$ samples having 5 wt.% alumina [19].

The coefficient of thermal expansion of alumina is about $8.4 \times 10^{-6}$ 1/°C and that of $B_4C$ and SiC are $5.5 \times 10^{-6}$ 1/°C and $2.4 \times 10^{-6}$ 1/°C, respectively.

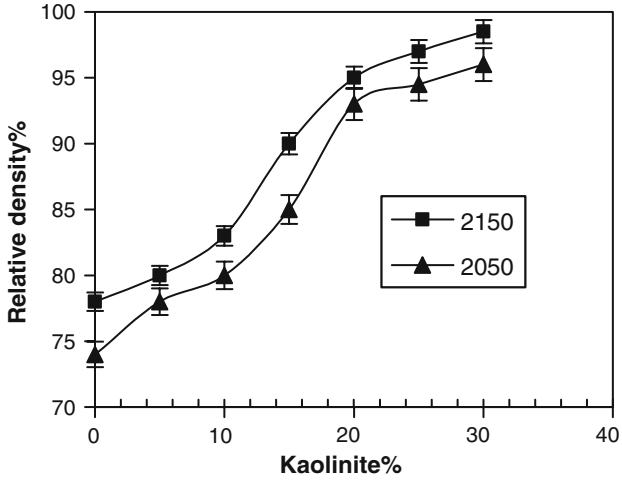


**Fig. 5** Effect of kaolinite addition on relative density of the samples sintered at 2150 °C (■) and 2050 °C (▲)

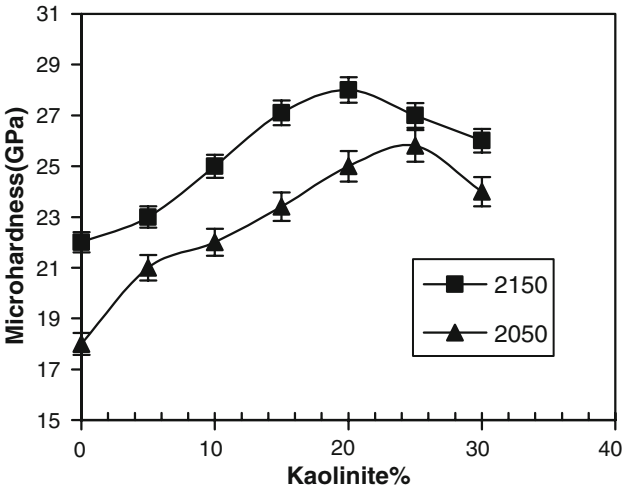


**Fig. 6** Effect of kaolinite addition on Vickers microhardness of the samples sintered at 2150 °C (■) and 2050 °C (▲)

The thermal expansion mismatch between constituents will cause stress network between $B_4C$ grains that lead to microcracks resulting in lowering the hardness.

The improved flexural strength and toughness can be related to reduction of porosity that is the main source of crack initiation. Moreover, by formation of alumina and SiC, some residual stresses exist in the samples that enhance these properties by crack deflection and microcracking mechanisms (Ref 19). It seems that in the present study the same phenomenon controls the mechanical properties.

## 4. Conclusions

1. The addition of kaolinite has a beneficial effect on sinterabillity and density improvement of the $B_4C$ material.
2. The mechanical properties, except hardness, improve by addition of kaolinite up to 30 wt.% to starting $B_4C$ powder. Hardness, first increases for samples having up to 20 wt.% kaolinite and then decreases for samples having higher amounts of kaolinite.

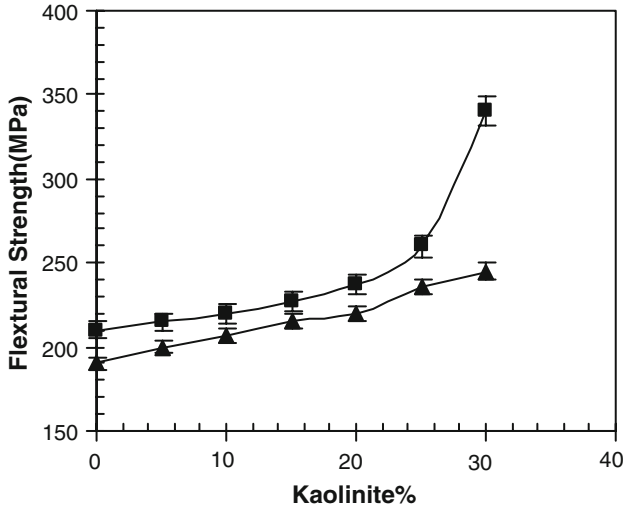


**Fig. 7** Effect of kaolinite addition on flexural strength of the samples sintered at 2150 °C (■) and 2050 °C (▲)

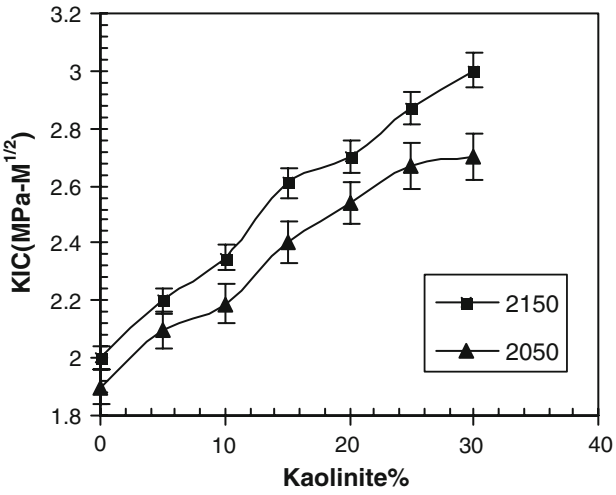


**Fig. 8** Effect of kaolinite addition on fracture toughness of the samples sintered at 2150 °C (■) and 2050 °C (▲)

3. The improvement of toughness is mostly due to a decrease in the porosity in the samples. It is also hypothesized that the presence of less hard phases in the matrix and residual stresses around $Al_2O_3$ and SiC phases are other possible causes of the enhanced toughness.


### Acknowledgments

The authors would like to thank Malek Ashtar, University of Technology and University of Tehran for supporting the present project.


### References


1. C.C. Philip, Ceramic Composites Containing Spinel Silicon carbide, and Boron Carbide, European Patent No. 921085924, 1999
2. G. Magnani, G. Beltrani, and G. Loris, Pressureless Sintering and Properties of a SiC-B4C Composites, *J. Eur. Ceram. Soc.*, 2001, **21**, p 633–638

3. G.Q. Weaver, Sintered High Density Boron Carbide, US Patent No. 4320204, 1982
4. L.S. Sigl, Processing and Mechanical Properties of Boron Carbide Sintered with TiC, *J. Eur. Ceram. Soc.*, 1998, **18**, p 1521–1529
5. T. Vasilos and S.K. Dutta, Low Temperature Hot Pressing of Boron Carbide and its Properties, *Am. Ceram. Soc. Bull.*, 1974, **53**, p 435–438
6. H. Lee and R. F. Speyer, Pressureless Sintering of Boron Carbide, *J. Am. Ceram. Soc.*, 2003, **86**(9), p 1468–1473
7. R.F. Speyer and H. Lee, Advances in Pressureless Densification of Boron Carbide, *J. Mater. Sci.*, 2004, **39**(19), p 6017–6021
8. M. Bougoin and F. Thevenot, Pressureless Sintering of Boron-Carbide with an Addition of Polycarbosilane, *J. Mater. Sci.*, 1987, **22**(1), p 109–114
9. S.L. Dole, S. Prochazka, and R.H. Doremus, Microstructural Coarsening During Sintering of Boron-Carbide, *J. Am. Ceram. Soc.*, 1989, **72**(6), p 958–966
10. A. Goldstein, Y. Geffen, and A. Goldenberg, Boron Carbide-Zirconium Boride in situ Composites by the Reactive Pressureless Sintering of Boron Carbide-Zirconia Mixtures, *J. Am. Ceram. Soc.*, 2001, **84**(3), p 642–644
11. Niihara, Process for Forming a Sintered Composite Boron Carbide Body, US Patent No. 5, 637,269, 1996
12. D. Stibbs, C.G. Brown, and R. Thompson, Dense Sintered Boron Carbide Containing Beryllium Carbide, US Patent No. 3146571, 1973
13. S. Prochazka, Sintering Boron Carbide Containing Beryllium Carbide, US Patent No. 4005235, 1997
14. A.K. Kundsen and W. Rafaniello, Titanium Diboride/Boron Carbide Composites with High Hardness and Toughness, US Patent No. 4957884, 1990
15. T. Graziani and A. Bellosi, Production and Characteristics of $B_4C/TiB_2$ Composites, *Key Eng. Mater.*, 1995, **104–107**, p 125–132
16. K.-F. Cai and C.-W. Nan, The Effect of Silicon Addition on Thermoelectric Properties of a $B_4C$ Ceramic, *Mater. Sci. Eng. B*, 1999, **67**, p 102–107
17. L. Levin, N. Frage, and M.P. Darriel, The Effect of Ti and $TiO_2$ Addition on the Pressureless Sintering of $B_4C$, *Metall. Mater. Trans. A*, 1999, **30**(12), p 3201–3210
18. C.C. Wu and R.W. Rice, Porosity Dependence of Wear and Other Mechanical Properties on Fine-grain Alumina and Boron Carbide ($B_4C$), *Ceram. Eng. Sci. Proc.*, 1985, **6**, p 977–994
19. H.-W. Kim, Y.-H. Koh, and H.-E. Kim, Densification and Mechanical Properties of $B_4C$ with $Al_2O_3$ as a Sintering Aids, *J. Am. Ceram. Soc.*, 2000, **83**(11), p 2863–2865
20. V.V. Shorokhod, M.D. Vlajic, and V.D. Kristic, Pressureless Sintering of $B_4C$-$TiB_2$ Ceramic Composites, *Mater. Sci. Forum*, 1998, **282–283**, p 219–224
21. S. Yamada, K. Hirao, and S. Sakaguehi, Microstructure and Mechanical Properties of $B_4C$-$CrB_2$ Ceramics, *Key Eng. Mater.*, 2002, **206–213**, p 811–814
22. ASTM B311-93, Test Method for Density Determination for Metallurgy (P/M) Materials Containing less than Two Percent Porosity, 2002
23. ASTM C1495-01, Test Method for Effect of Surface Grinding on Flexure Strength of Advanced Ceramics, 2002
24. ASTM C1161-01, Test Method for Flexure Strength of Advanced Ceramics at Ambient Temperature, 2002
25. Military Standard MIL-STD-1942A-93, Test Method for Flexure Strength of High Performance at Ambient Temperature, 1990
26. P. Chantikul and G.R. Lawn, A Critical Evaluation of Indentation Techniques for Measuring Fracture Toughness, I. Direct Crack Measurement, *J. Am. Ceram. Soc.*, 1981, **64**, p 539–543
27. D. Casellas, I. R_Afols, L. Lianes, and M. Anglada, Fracture toughness of zirconia-alumina composites, *Int. J. Refract. Metals Hard Mater.*, 1999, **17**, p 11–20